BBA - Biomembranes 1866 (2024) 184290

Contents lists available at ScienceDirect

BBA - Biomembranes

journal homepage: www.elsevier.com/locate/bbamem

Extracellular membrane vesicles derived from *Komagataeibacter oboediens* exposed on the International Space Station fuse with artificial eukaryotic membranes in contrast to vesicles of reference bacterium

I. Orlovska [a], G. Zubova [a,*], O. Shatursky [b], O. Kukharenko [a], O. Podolich [a], T. Gorid'ko [b], H. Kosyakova [b], T. Borisova [b], N. Kozyrovska [a]

[a] *Institute of Molecular Biology and Genetics of NASU, Acad. Zabolotnoho str, 150, Kyiv 030143, Ukraine*
[b] *Palladin Institute of Biochemistry of NASU, Leontovycha str, Kyiv 01024, Ukraine*

ARTICLE INFO

Keywords:
Extracellular membrane vesicles
Planar bilayer lipid membrane
Pore-forming
Fusion
Lipids
Protein aggregates

ABSTRACT

Membranous Extracellular Vesicles (EVs) of Gram-negative bacteria are a secretion and delivery system that can disseminate bacterial products and interact with hosts and the environment. EVs of nonpathogenic bacteria deliver their contents by endocytosis into eukaryotic cells, however, no evidence exists for a fusion delivery mechanism. Here, we describe the fusion of exposed to space/Mars-like stressors simulated on the International Space Station vesicles (*E*-EVs) from *Komagataeibacter oboediens* to different types of model planar membranes in comparison with the EVs of the ground-based reference strain. The most reliable fusion was achieved with PC:PE: ergosterol or sterol-free PC:PE bilayers. The relative permeability ratio (PK+/PCl-) estimated from the shift of zero current potential according to Goldman–Hodgkin–Katz equation consisted of 4.17 ± 0.48, which coincides with preferential cation selectivity of the EV endogenous channels. The increase in membrane potential from 50 mV to 100 mV induced the fusion of *E*-EVs with all tested lipid compositions. The fusion of model exosomes with planar bilayer lipid membranes was confirmed by separate step-like increases in its conductance. In contrast, the ground-based reference *K. oboediens* EVs never induced the fusion event. In our study, we show membrane lipidome perturbations and increased protein aggregation occurred in the exposed samples in the harsh environment when outer membranes of *K. oboediens* acquired the capability of both homo- and heterotypic fusion possibly by altered membrane fluidity and the pore-forming capability.

1. Introduction

Nanoscale extracellular vesicles (EVs) comprise heterogeneous populations of naturally occurring biological nanoparticles that cells of all living organisms produce under physiological and pathological conditions [1]. They are called exosomes and membranous nanoparticles in eukaryotes [2], outer-membrane vesicles in Gram-negative bacteria, membrane vesicles in Gram-positive bacteria and archaea [3,4]. These EVs play a significant role in intercellular communication by serving as a carrier for membrane and cytosolic proteins, lipids, DNA and RNA species between cells [5]. Bacterial EVs are seen as having enormous potential in biomedical applications in theranostics [6,7]. In particular, EVs are considered a novel therapeutic approach in patients with intestine problems [8] and osteoporosis [9]. EVs' capacity to deliver therapeutics to hard-to-reach tissues makes them ideal for drug delivery to the brain, solid tumors or hair cells [9,10]. Importantly, bacterial EVs are naturally immunogenic, making them attractive for vaccine design [11,12], and therefore, they have a promising future for Astrobiomedicine as edible vaccines and nano drugs [13,14]. The rising therapeutic interest in EVs is linked to their capacity to internalize molecular cargo to various types of cells. EVs can transfer their content by being phagocytosed, micropinocytosed or endocytosed [15]. The transfer of molecules from EVs of pathogenic bacteria to target cells can occur *via* the direct fusion of EVs with the plasma membrane of the recipient cell [16,17]. The fusion of bacterial EVs to host membranes is involved in transmitting virulence factors in non-phagocytic cells and

* Corresponding author.
E-mail addresses: i.vviki@ukr.net (I. Orlovska), anka.kiev@gmail.com (G. Zubova), olegshatursky@biochem.kiev.ua (O. Shatursky), hikia48@gmail.com (O. Kukharenko), podololga@ukr.net (O. Podolich), tangori@ukr.net (T. Gorid'ko), kosiakova@hotmail.com (H. Kosyakova), tatianabiochem@gmail.com (T. Borisova), kozyrna@ukr.net (N. Kozyrovska).

https://doi.org/10.1016/j.bbamem.2024.184290
Received 3 August 2023; Received in revised form 10 January 2024; Accepted 22 January 2024
Available online 26 January 2024

reprogramming phagosomes in phagocytic macrophages [18]. The modified vesicle membrane structure (*e.g.*, with an enhanced fusion of EV populations or incorporation capacity) is the focus of translation medicine research. To date, there is a single report of induced fusion of non-pathogenic bacterial EVs: a higher fusion rate of bacterial EVs has been achieved with decreased pH and increased salt concentration [19].

Here, we show that membrane vesicles from *Komagataeibacter oboediens* - a member of kombucha multimicrobial community - exposed to stressful conditions of spaceflight (*E*-EVs) [20,21], successfully fused with artificial phospholipid bilayer membranes (BLM) that mimic eukaryotic ones without application of osmotic gradient or physiologically significant divalent cations. In contrast, EVs from reference bacterial species *K. oboediens* probably have no mechanism to fuse with synthetic membranes. We show lipidome perturbations and increased protein aggregation occurred in membranes under the exposure of samples in the harsh environment that perhaps play key roles in the *E*-EV fusion capability.

2. Materials and methods

2.1. Isolation of bacterial and amniotic extracellular vesicles

Cellulose-producing bacteria were isolated from the exposed to space/Mars-like conditions kombucha samples and identified as *K. oboediens* IMBG185, and the isolate from a reference ground-based sample - *K. oboediens* IMBG180 [22]. Both strains were cultured in HS medium [23] at 28 °C for three days and undergone by serial centrifugation at 10,000 and 17,000 rpm for 20 min at 4 °C, followed by ultracentrifugation at 100,000*g* for 1 h at 4 °C (Beckman Instruments Inc., L8M, rotor 55.2 Ti). The resulting pellet was re-suspended in sterile filtered (0.20 μ pore size filter; Minisart, Sartorius, Germany) phosphate-buffered saline, pH 7.4. Human amniotic fluid samples were obtained sterilely from informed, healthy volunteers at the C-section. The amniotic fluid was spun at 3000 rpm for 5 min at 4 °C and used for exosome isolation. Sterile concentrated samples were stored at -80 °C.

2.2. Characterization of EVs

2.2.1. Visualization of isolated vesicles

Visualization of isolated vesicles was performed using dynamic light scattering (DLS), transmission electron microscopy (TEM) and scanning electron microscopy (SEM), as previously described [20]. The size distributions of EVs were determined by analysis of the intensity of light scattering at 25 °C using Nano-ZS machine (Malvern, UK) and the software (Zetasizer ver. 7.03, Malvern, UK).

2.2.2. Assessment of membrane lipidome of extracellular vesicles

The total phospholipid content of EVs was determined as previously described [24]. The Carlo Erba HRGC, 5300 gas chromatograph (Italy) with flame ionization detector equipped with a glass-packed column (length – 3.5 m, internal diameter – 3.0 mm) completed with 10 % SP-2300 phase (Silar 5CP) on Chromosorb W/HP, was used to separate and identify fatty acid methyl esters. The temperature was programmed from 140 to 250 °C, at 2 °C/min, with a final hold. The Agilent Technologies 7890A gas chromatograph (USA) with SP-2560 column (100 M × 0,25 MM, df 0.20 μm, Germany) was used to separate and identify cis/trans isomers of unsaturated fatty acids methyl esters. The temperature was programmed from 140 to 240 °C, at 4 °C/min, with a final hold. Individual fatty acids in samples were identified based on their retention time compared to appropriate commercially available standards (Sigma-Aldrich, USA; Serva, Germany). Results were expressed as a percentage of total fatty acids. All the experiments were repeated three times.

2.3. Measurement of Ca^{2+}-dependent fusion

Homotypic fusion capability of EVs isolated from kombucha microbial community (KMC) samples exposed to the hybrid space/Mars-like environment at the top level of Tray 2 with native kombucha vesicles (100 μg/mL of protein) was initiated by the addition of Ca^{2+} (2 mM), controlled with Zeta Sizer Nano ZS (Malvern, UK), measuring dynamic light scattering (DLS). Heterotypical fusion events of EVs of *K. oboediens* isolated from exposed and reference KMCs modelled in PBS (pH 7.4) in the presence of Ca^{2+} (2 mM). The size of hybrid (or aggregated) vesicles was measured with DLS.

2.4. Fusion of the vesicles with a planar lipid bilayer

The fusion of the vesicles with a planar phospholipid membrane was assessed by monitoring vesicle-induced transmembrane current in BLMs [25,26]. The lipid bilayers were formed from the solution of cholesterol (Avanti Polar Lipids, Alabaster, AL, USA) or ergosterol (Sigma-Aldrich Chemie GmbH, Steinheim, Germany) and phospholipids: phosphatidylcholine (PC; Biolik, Ukraine), phosphatidylethanolamine (PE), 1,2-diphytanoyl-sn-glycero-3-phosphocholine (DPhPC) (Avanti Polar Lipids, Alabaster, AL, USA). The mixtures of sterol and phospholipids were maintained at a weight ratio of 1/1/0.385 for PC:PE:ergosterol, PC:PE:cholesterol, DPhPC:PE:cholesterol, DPhPC:PE:ergosterol or 1/2 for cholesterol:PC and ergostero:DPhPC l at the total lipid concentration in n-heptane solution of 20 mg/mL Bilayer membranes were painted across a round aperture in a thinned wall of a Delrin cup (0.15 mm diameter, Warner Instruments, Inc., USA) with a working volume of 1 mL held within a glass chamber. The membrane washing solution contained 10 mM Tris–HCl (pH 7.4) and the required quantities of potassium chloride (Sigma-Aldrich Chemie GmbH, Steinheim, Germany). The membrane-separated chambers could be stirred when needed. Voltage-clamp recordings of transmembrane current were made with a high-resolution amplifier BBA-02 (Eastern Scientific, LLC, Rockville, USA). Membrane-separated chambers were connected to HS-2 head-stage of the amplifier BBA-02 through a pair of agar bridges immersed into a 2 M KCl solution with silver chloride electrodes EAG-02 (Eastern Scientific, LLC, Rockville, USA). Voltage-ramp protocols of 60 mV/min or holding potentials within the range of ±100 mV were applied by universal signal generator RG-3 (Eastern Scientific, LLC, Rockville, USA) or voltage-source built-in amplifier BBA-02. Vesicles (2 mg/mL of protein) were introduced to the Delrin cup. The potential difference was referenced to the vesicle-free outer glass chamber, defined as being at ground potential. Transmembrane currents were filtered at 100 Hz and recorded by a computer through USB Digitizer Model ADA-1210 (Eastern Scientific, LLC, Rockville, USA) using Cole-Palmer Instrument Company software (Illinois, USA). The computer-made records were analyzed with Origin Pro 8.6.0 software. All experiments were conducted at room temperature (20–24 °C). Hereafter, mean values±standard deviations were indicated for 10–20 experiments, each made on a newly brushed bilayer.

2.5. Fluorescence spectroscopy

A fluorescent membrane probe, NR12S (a Nile Red-based compound), has been selected because of its sensitivity to hydration and polarity of the microenvironment [27]. This parameter characterizes the ratio of lipid-ordered and lipid-disordered phases in membranes and could be detected as the emission ratio of NR12S probe at 560 and 630 nm [27]. For staining, an equal volume of 0.04 μM NR12S, diluted *ex tempore* in Ringer's solution (in mM: 125 NaCl, 5 KCl, 1 $MgSO_4$, and 32 HEPES/NaOH (pH 7.4), 5 glucose, and 1 $CaCl_2$), was added to EVs or *E*-EVs and incubated in the dark at room temperature for 20 min. Since the probe has a low quantum yield in water-based buffers, there is no need in further washout [27,28]. Fluorescence signal was detected with PTI QuantaMaster 40 spectrofluorometer at 520 nm excitation. All the spectra were corrected for the fluorescence of the corresponding blank (suspension of vesicles without the probe).

2.6. Detection of amyloids

Amyloids were detected with the help of 1 % Theoflavin-T [29] in the preparation of bacterial culture for a "squeezed drop" type microscopy: a drop of the Theoflavin-T working solution and cells of the experimental culture in 2 repetitions were applied to the slides. All samples were covered with coverslips and kept for ten min in a closed container without access to daylight.

2.7. Statistical analysis

Results on membrane lipidome analysis and amyloids detection were expressed as mean ± standard deviation (SD) of independent experiments performed in triplicate. Two-tailed Student's *t*-test compared the difference between groups. The differences were considered to be significant, if $P \leq 0.05$. The computer-made records of transmembrane currents were analyzed with Origin Pro 8.6.0 software.

3. Results

3.1. Morphology and size distribution of extracellular vesicles used for fusion experiments

EV samples from the ground-based wild-type reference bacterial strain displayed average sizes recorded by DLS of 65 ± 0.3 nm, compared to larger *E*-EVs from the exposed *K. oboediens* (70 ± 0.5 nm). The DLS data agreed with the data obtained from the SEM micrographs of EVs (Fig. 1A, B). Their zeta potentials were −5.5 mV (wt EVs) and -1.5 mV (E-EVs), respectively. Amniotic fluid EVs distributed in the 30–80 nm range and exhibited characteristic pairs (Fig. 1C, D).

3.2. Fusions of bacterial EVs

Our previous research has reported that *K. oboediens* EVs and E-EVs could incorporate with the host cell *in vitro* [21]. However, the mechanisms of vesicle entry were not assessed. In addition, we have found that extracellular vesicle membrane lipidome has perturbations after the exposure of the KMC on the International Space Station. In particular, the amount of total lipids increased and unsaturated fatty acids decreased. The fusion as a putative mechanism of bacterial membrane vesicle incorporation in host cells may be predicted as one known.

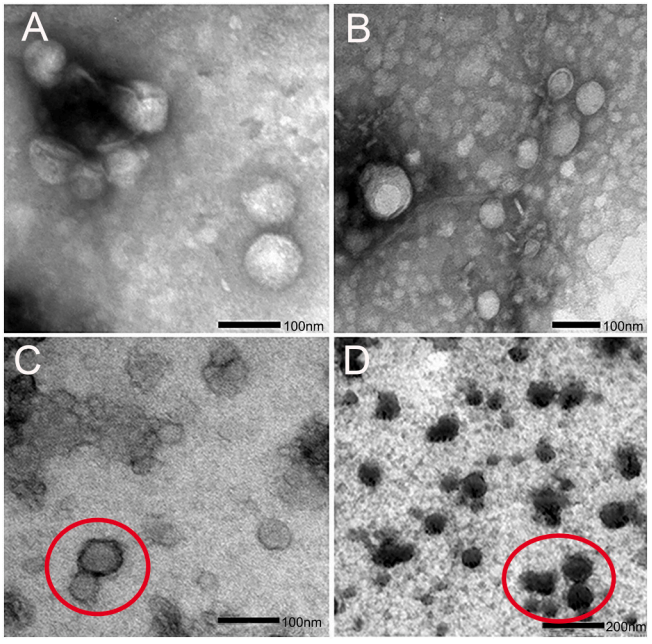

Fig. 1. Morphology of extracellular vesicles originated from *Komagataeibacter oboediens* IMBG185 exposed to the spaceflight/Mars-like conditions (A) and wild-type bacteria *K. oboediens* IMBG180 (B) (scanning electron microscopy) and amniotic fluid exosomes (C, D) (transmission electron microscopy). Circles indicate the characteristic arrangement of exosomes in pairs.

3.2.1. Ca^{2+}-dependent fusion of vesicles derived from kombucha microbial community

The fusion capability of vesicles isolated from the KMC sample exposed to the hybrid space environment compared to EVs of native culture served as a ground-based reference and demonstrated a significant increase in the size of vesicles in microbial populations, especially after Ca^{2+} application. This fact demonstrated that vesicles isolated from the KMC exposed to the space/Mars-like environment probably intensively fused with each other (Fig. 2A, B), also in response to the addition of Ca^{2+} to the incubation buffer (Fig. 2B). In EVs of control culture (Fig. 2C), only insignificant changes in the vesicles size in populations were registered even after Ca^{2+} application (Fig. 2D).

3.2.2. Fusion of E-EVs with exosomes

The heterotypic fusion of E-EV samples from bacteria *K. oboediens* IMBG185 isolated from exposed KMC samples with exosomes isolated from the amniotic fluid is shown in Fig. 2E-H. The fusion events

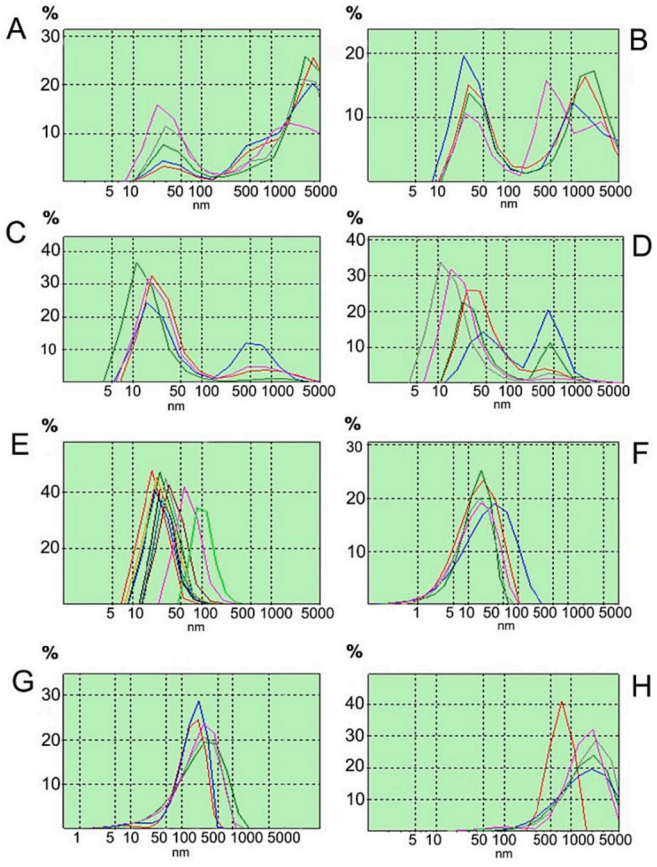

Fig. 2. The homotypic (A-D) fusion of extracellular membrane vesicles (EV) originated from kombucha microbial culture (KMC) samples exposed to hybrid space/Mars-like stressors on the International Space Station (*E*-EV) (A) and after a fusion induced with Ca2+ (B); reference ground-based KMC EVs (C) after a fusion induced with Ca2+ (D). The heterotypic fusion of exosomes with bacterial E-EVs (E-H); EVs from amniotic fluid (exosomes) (E); E-EVs from *Komagataeibacter oboediens* IMBG185 reisolated from exposed KMC (F); a fusion of exosomes with E-EVs (G); a fusion of exosomes with E-EVs stimulated with Ca2+ (H). The size of different populations of extracellular membrane vesicles was measured by using dynamic light scattering (Zetasizer Nano ZS).

probably took place after incubating both kinds of vesicles, as seen in the increase in vesicle sizes documented with DLS (Fig. 2G). More pronounced changes in the size of vesicles in populations were registered after applying Ca^{2+} (Fig. 2H).

However, the DLS data on the increase of vesicle sizes do not prove their fusion and do not exclude simple aggregation events. Our following assessment of the putative fusion capability of changed bacterial EVs included their interaction with the planar bilayer membranes.

3.3. Pore-formation induced by extracellular membrane vesicles in the planar phospholipid membranes

The planar phospholipid membrane model was selected to elucidate the fusion event as a probable mode of bacterial vesicle interaction with the eukaryotic cell membrane. The planar bilayers such as PC:PE: ergosterol, PC:PE:cholesterol, DPhPC:PE:cholesterol, DPhPC:PE:ergosterol, PC:cholesterol and sterol-free PC:PE were composed, and fusions of the EVs samples with these bilayers were supposed to be confirmed by discrete step-like increases in BLM conductance due to formation of endogenous channels in the planar phospholipid membrane as described earlier [25,26,30].

3.3.1. Pore-formation induced by bacterial vesicles in the planar phospholipid membranes

The formation of stable ion-conducting pores in the planar bilayer was registered on the transmembrane current increase after the addition of the *E*-EVs sample inside the Delrin cup (Fig. 3A, left inset), while the addition of EVs at the same concentration never resulted in a stable appreciable increase of transmembrane current (Fig. 3, right inset). The *E*-EV-induced transmembrane current rose readily after a lag time of 1–15 min, depending upon the lipid composition of BLM, as the positive potential (+50 mV; +100 mV) was applied to the vesicle-containing side of the membrane. However, the increase in the E-EV-induced current was also observed when physiologically relevant positive potential (+50 mV; +100 mV) was applied to the membrane side opposite the vesicle-containing diluent (data not shown). It suggests that membrane polarization is unnecessary for pore-formation driven by the E-EVs sample with the BLM. However, the negative potential applied to the vesicle-containing side of the membrane reduced the time lag necessary for inserting endogenous channels from *E*-EVs into the planar membrane. While the increase in conductance of the *E*-EVs-treated cholesterol-containing PC, DPhPC and PE:PC BLMs was retarded, the readiness of E-EVs to fuse with planar membrane increased significantly on the BLMs formed from PC:PE:ergosterol or PE:PC, thus reducing pre-insertion lag time to 1–2 min.

The step-conductance displays a wide distribution, ranging from 60 pS to 8 nS (Fig. 3B, left inset) with a peak at approximately 62 ± 15 pS as, probably, does the vesicle size, unless the larger separate increases in current occurred due to simultaneous insertion of channels from the package of smaller size vesicles.

The rise of transmembrane current achieved on PC:PE:ergosterol, PC: PE:cholesterol, DPhPC:PE:cholesterol, DPhPC:PE:ergosterol, PC:cholesterol and PE:PC bilayers by *E*-EVs either reached a steady-state or was stopped by washing-out with vesicle-free saline and also remained stable. This suggests that the fusion of *E*-EVs with all types of planar membranes was irreversible. However, the most reliable fusion was achieved with PC:PE:ergosterol or sterol-free PC:PE bilayers. The ability of E-EVs to fuse with PC:PE:ergosterol or sterol-free PC:PE bilayers allowed to achieve a readily increasing transmembrane current without conventional application of trans-bilayer osmotic gradient or one-sided addition of physiologically significant divalent cations.

The steady-state transmembrane current induced by *E*-EVs reversed at −29.95 ± 3.8 mV in the membrane washing solution of 100 mM KCl on the vesicle addition side and 10 mM KCl on the opposite side (Fig. 3A, curve 2). Hence, the relative permeability ratio (PK+/PCl-) estimated from the shift of zero current potential according to Goldman–Hodgkin–Katz equation consisted of 4.61 ± 1.28, which suggests a weak cation selectivity of summary current induced in the BLM by E-EVs endogenous channels.

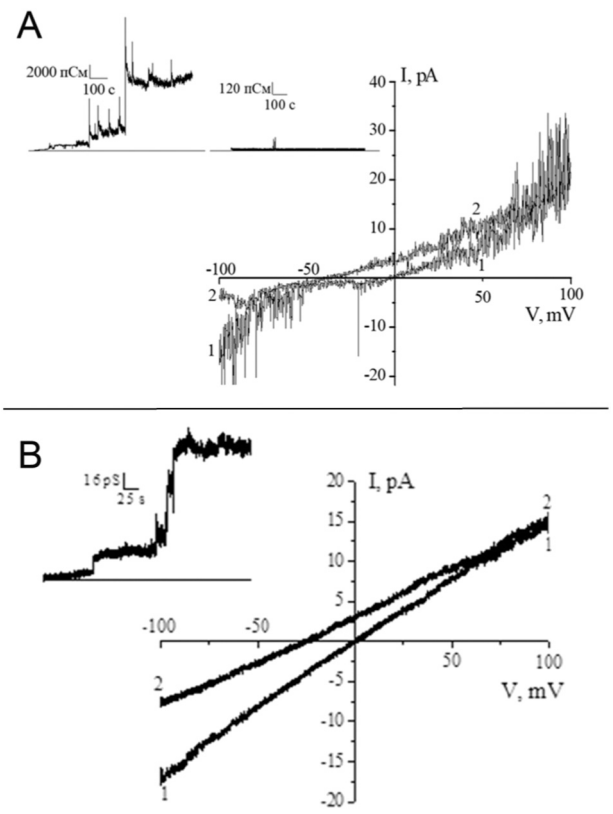

Fig. 3. Typical records of transmembrane current across PC:PE:ergosterol planar bilayer resulted from the fusion with E-EV (originated from bacteria *Komagataeibacter oboediens* exposed on the International Space Station) (A) and the reference vesicles fraction (originated from human amniotic fluid, HAF) (B) upon the membrane potential and 10-fold transbilayer salt gradient. A, Curve 1 - the membrane-separated solution of 100 mM KCl; curve 2 - current-voltage relationships after consecutive replacement of 100 mM KCl for 10 mM KCl on the side of membrane opposite to which the potential and E-EV vesicles were applied. (Inset, left panel) Increase in transmembrane current after the addition of E-EV vesicles into a Delrin cup at +50 mV membrane potential. (Inset, right panel) Transmembrane current after the addition of the reference vesicle fraction (originated from reference ground-based bacteria *K. oboediens*) into a Delrin cup at +50 mV membrane potential. B, Typical dependence of stationary current across PC:PE:ergosterol planar bilayer (weight ratio of 1/1/0.385) resulted from the fusion with HAF exosomes upon the membrane potential and 10-fold trans-bilayer salt gradient. Curve 1 - the membrane-separated solution of 100 mM KCl; curve 2 - current-voltage relationships after consecutive replacement of 100 mM KCl for 10 mM KCl on the side of the membrane opposite to which the potential and HAF exosomes were applied. (Inset) Increase in transmembrane current after the addition of HAFE into a Delrin cup at +100 mV membrane potential.

The application of 5 mM $CdCl_2$ onto an E-EVs-induced steady-state current decreased the inward current approximately by 70 % in the symmetric solution of 100 mM KCl at the potential of +50 mV applied to the vesicles-containing chamber (data not shown). The binding of cadmium ions with the negatively charged ionogenic groups in the endogenous channel interior is also consistent with the cationic selectivity of E-EVs-induced transmembrane current.

3.3.2. Pore-formation induced by human amniotic fluid exosomes (HAFE) in the planar phospholipid membranes

HAFE were chosen to experimentally show the fusion of representatives of native eukaryotic membranes with artificial ones that mimic

them. Here, this model served as a positive control for the prokaryotic vesicle fusion experiment. The fusion of HAFE with planar bilayer (PC:PE:ergosterol) was confirmed by separate step-like increases in BLM conductance due to the insertion of endogenous channels from the vesicle membrane following the fusion events. The exosome-induced transmembrane current increased appreciably within a 5 min lag time at the positive voltages (+50 mV; +100 mV) applied to the vesicle-containing side of the membrane washed in an asymmetric solution of 100 mM KCl on the vesicles addition side and 10 mM KCl on the opposite side of the planar membrane (Fig. 3B, inset). The increase in exosome-induced current was also observed when physiologically relevant positive potential (+50 mV; +100 mV) was applied to the membrane side opposite the vesicle-containing chamber (data not shown). This suggests that membrane polarization is not a necessary prerequisite for pore-formation driven by exosome fusion, just as it occurred with the *E*-EV fusion described above.

The rise of exosome fraction-created transmembrane current achieved on PC:PE:ergosterol, DPhPC:PE:cholesterol, DPhPC:PE:ergosterol, PC:cholesterol and PE:PC bilayers either reached a steady state or was stopped by washing-out with vesicle-free saline and also remained stable. This suggests that the fusion of exosomes with these planar membranes and insertion of endogenous channels were irreversible, although the most reliable fusion was achieved with PC:PE:ergosterol or sterol-free PC:PE bilayers. The ability of exosomes to fuse with PC:PE:ergosterol or sterol-free PC:PE bilayers allowed to achieve a readily increasing transmembrane current without the application of trans-bilayer osmotic gradient (data not shown) although the creation of a 10-fold salt gradient increased the number of fusion events and reduced the time lag before the fusion with BLMs. The increase in membrane potential from 50 mV to 100 mV also increased the fusion events of exosomes with all types of BLMs used in this study.

The current-voltage relationship of exosome-induced current was determined by the application of a voltage ramp onto a steady-state transmembrane current (Fig. 3B, curves 1,2). The application of steadily increasing negative voltages slightly rectified the steady-state macroscopic current, raising 1.2 times more current at −100 mV than at +100 mV applied to the vesicle-containing chamber (Fig. 3B, curve 1). Thus, unlike the potential dependency of transmembrane current induced by *E*-EVs (Fig. 3A, curve 1), the asymmetry coefficient obtained for stationary current created by fusion with exosomes suggested the increase in inward current.

3.4. Bacterial vesicle membrane lipid composition before and after exposure to stressors

The membrane of the cellulose-synthesizing bacteria *Komagataeibacter* spp. (acetic acid bacteria) possess an unusual membrane lipid composition that includes, *e.g.*, sphingolipids and hopanoids (functional

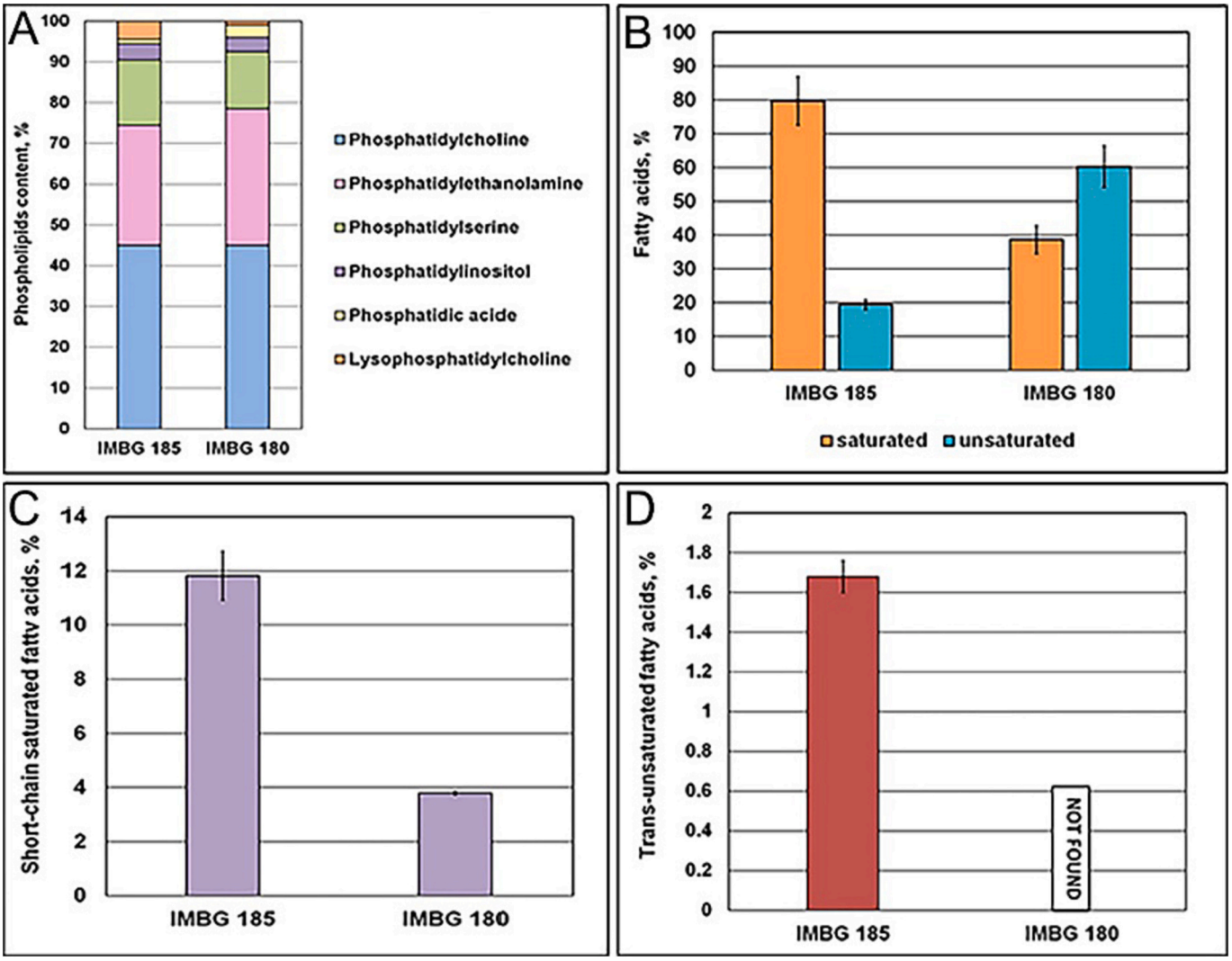

Fig. 4. Phospholipids (A) and fatty acids (B-D) of extracellular membrane vesicles of the *Komagataeibacter oboediens* cultures: IMBG185, exposed to hybrid space/Mars-like environment simulated on the International Space Station; IMBG180, ground-based reference. Data are presented as the mean ± SD ($n = 3$), $p \leq 0.05$.

analogues of cholesterol in bacterial membranes) [31], probably because they can grow at low pH. After the exposure of bacteria under space/Mars-like stressors on the ISS, the amount of some anionic PLs (phosphatidylserine, lysophosphatidylcholine, phosphatidylinositol) increased, being affected by stressors (Fig. 4A). The free fatty acid (FA) content of *E*-EVs isolated from the *K. oboediens* IMBG185 increased significantly, compared to the untreated control IMBG180 (Fig. 4B-D). The quantity of total saturated FA had 1.7–2 fold ($p < 0.05$) increases while unsaturated FA (mainly monounsaturated) decreased 2.5–3.1-folds ($p < 0.05$) in E-EVs, in contrast to reference type EVs (Fig. 4B). The exposure of *K. obedience* caused the appearance of short-chain saturated fatty acids (C6:0 – C11:0) and trans FAs - elaidic (18:1w9) and linolelaidic (18:2w6) in the E-EVs (Fig. 4C, D).

3.5. Fluorescence of NR12S in bacterial EV membrane

Probe NR12S can directly address the lipid order in the membrane by variation in the excitation maximum as it binds exclusively to the outer membrane leaflet. The changes of the lipid order in the vesicle membranes was determined by the fluorescent signal of the NR12S probe. In IMBG185, the fluorescence emission of NR12S was significantly shifted towards longer wavelengths when compared to IMBG180 (Fig. 5A). It exhibits a significant shift in the liquid-ordered phase where phospholipids with saturated acylic chains enriched with cholesterol-like (in bacteria) in the membranes of exposed bacteria vesicles as compared to the liquid-disordered phase (mainly the phospholipids with unsaturated acylic chains) characteristic for the membranes of ground control bacteria and vesicles. Notably, bacterial membranes lacking cholesterol cannot be described in terms of liquid-ordered and liquid-disordered phases, but only in terms of higher or lower lipid order [32].

3.6. Formation of amyloid proteins in K. oboediens under the impact of the stressors

It is known that amyloids are produced by microorganisms in small quantities during the folding process, and their yield under adverse environmental conditions may increase [33]. Oligomers create membrane pores in bacteria [34]. In the study of biofilm-forming bacteria *K. oboediens*, we found that after exposure to stressors for a long time, experimental culture in subsequent generations retained an enhanced ability to produce protein aggregates. Numerous cells with fluorescence were found in the sample of *K. oboediens* IMBG185 after binding Thioflavin T dye (Fig. 5Bb). Fluorescent zones, which indicated the presence of amyloids in *K. oboediens* IMBG180 without stress, were single (Fig. 5Ba), exhibiting so far significant difference in amyloid proteins rate produced by *K. oboediens* bacteria, dependent on the influence of stressors (Fig. 5C).

4. Discussion

The process of phospholipid vesicle fusion with membranes depends on membrane lipid composition and shape [35] and fusogen proteins [36]. In this study, we show the difference between the wild-type and modified EVs in the mode of interaction with the artificial membrane that mimics the eukaryotic membrane. In particular, *E*-EVs derived from bacteria that were exposed to harsh environmental conditions displayed the formation of pores in the planar bilayers, *i.e.*, exhibited membrane unification and a fusion event. In contrast, EVs from untreated reference strain did not build pores in planar phospholipid membranes with known structures. We may predict that the changed lipid structure/shape in the *E*-EV membrane and a pore-forming component with high activity in lipid bilayers played a role in acquiring membrane fusion capability.

4.1. Changed membrane lipids composition as an attributor for membrane fusion

Under unfavorable conditions, membrane lipid bilayers undergo a reversible change of state from a fluid (disordered) to a nonfluid (ordered) state, depending on fatty acid acyl chain packing, which leads to differences in membrane fluidity [37]. For example, low fluidity triggers a lipid phase separation into a liquid-disordered phase in membranes [38]. However, biological membranes lacking cholesterol, *e.g.*, bacterial ones, which may include cholesterol-like compounds – hopanoids -

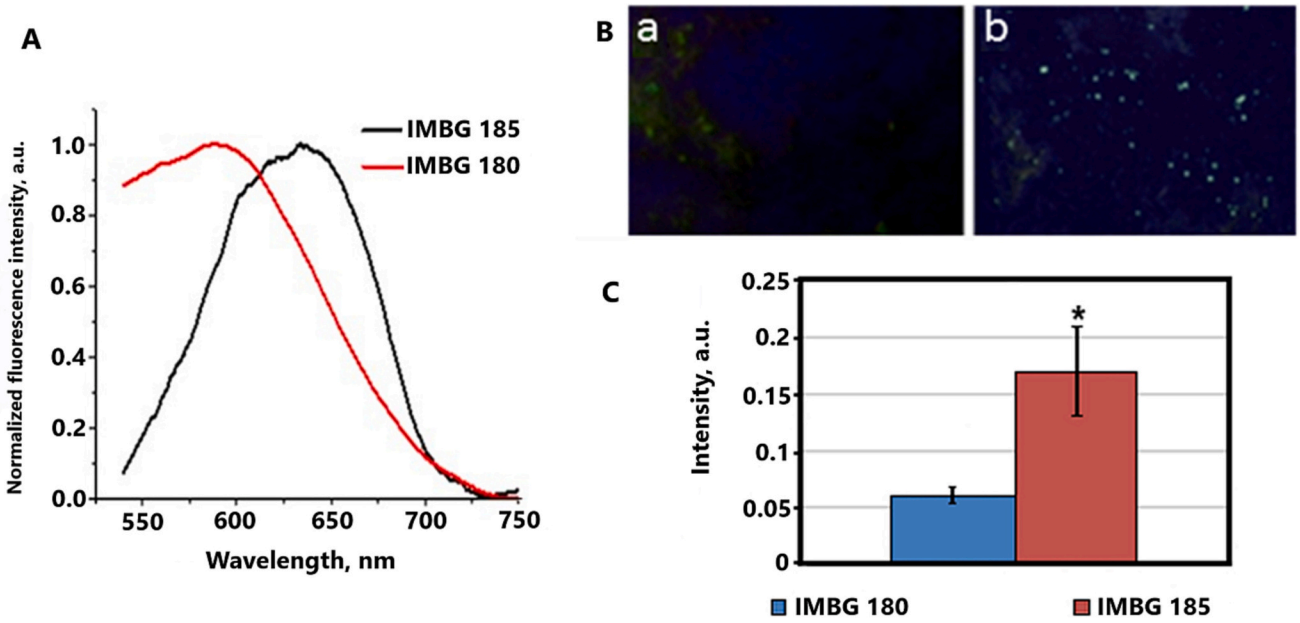

Fig. 5. Fluorescence emission spectra of the NR12S dye in outer-membrane vesicles of *Komagataeibacter oboediens* IMBG180 and IMBG185 (A) and amyloid proteins of *K. oboediens* bind to Thioflavin T dye (B, C). A, the NR12S probe shows changes in emission ratio (560 nm/630 nm) in outer-membrane vesicles of *K. oboediens* IMBG180 and IMBG185 as a function of lipid-ordered phase/lipid-disordered phase in membranes. B, the image of amyloid proteins of *K. oboediens* IMBG180 (Ba) and IMBG185 (Bb) bind to Thioflavin T dye. C, percentage of amyloid proteins produced by *K. oboediens* bacteria, depending on the influence of stressors. Data are presented as the mean ± SD ($n = 48$), $p \leq 0.05$.

cannot be described in terms of liquid-ordered and liquid-disordered phases, but only in terms of higher or lower lipid order [39].

Gohrbandt et al. [39] show that reduced membrane fluidity in *E. coli* cells causes reversible phase separation upon accumulation of saturated fatty acids to a content of 80 %. Previously, we showed that after the impact of the Mars-range UV, the increased synthesis of lipids, especially phospholipids and fatty acids, caused alteration in the membrane fluidity of the exposed bacteria [21]. In *E*-EVs of these bacteria, the content of total saturated fatty acids was 2-fold increased compared with reference bacterial membranes and reached 80 % (Fig. 4B). A significant shift towards longer wavelength corresponds to a lipid-ordered phasing, where phospholipids with saturated acylic chains are enriched in the membranes of exposed bacteria vesicles and correlates with the increase of the saturated fatty acids content in their membranes [21]. The noticed alterations in the cell membrane structure could lead to a changed mode of interaction with the eukaryotic-like membranes, *i.e.* to the fusion of their membranes. The unification of E-EVs with an exosome bilayer membrane documented by DLS and a pore registered by transmembrane current also confirm bacterial vesicle capacity to interact with eukaryotic membrane in the fusion mode. Increased content of lipids in E-EVs such as phosphatidylinositol and lysophosphatidylcholine, which generate intrinsic positive curvature in the inner leaflet of the membrane, could facilitate pore formation. The fact that the readiness of E-EVs to fuse with PC:PE:ergosterol planar membrane increased significantly compared to cholesterol-containing PC, DPhPC and PE:PC BLMs, may lead to a conclusion that in kombucha culture, which consists of bacteria and yeasts, changed interactions between E-EVs and yeasts may occur, as the latter contain ergosterol in their membranes [40].

Direct membrane fusion with host cell membranes, preferentially at lipid raft-like domains, has been reported to be a potential mechanism of bacterial EVs entry [16]. Normally, representatives of the domain Bacteria do not synthesize cholesterol, a player in lipid raft formation, however, some genera produce cholesterol-like compounds [31]. *K. oboediens* produces cholesterol-like species (hopanoids) *via* the expression of squalene hopene cyclase [22]. Nevertheless, lipid bilayers do not fuse naturally without perturbations of their organization and dynamics by any fusogen proteins [41]. In our study, bacterial membrane components, including proteins, were altered under space/Mars-like stressors simulated on the ISS, and that fact could be responsible for new capacity acquisition.

4.2. Peptide-induced change in the membrane, leading to fusion?

A big body of evidence exists on the observation that amyloidogenic proteins, such as Aβ, α-synuclein, *etc.*, are able to form pores or single channels in membranes *in vitro* [42–44], probably, using a common mechanism of a pore formation. Amyloid aggregation depends on the membrane-phase behavior [45]. In bacteria, a prion-like protein builds pores [34,46]. Damage to the membrane by toxic protein aggregates compromises bioenergetics, triggers oxidative stress, sequestration of proteins and scavenging ROS and therefore prevents the adequate cellular response [47,48] or causes failure in regulating plasma membrane proteins, such as receptors and ion pumps. At the same time, these protein aggregates play a functional role in bacteria [49], *e.g.*, they can contribute to adhesion, biofilm formation, genetic competence, cell density regulation, and interactions with hosts. In the "channel hypothesis", the formation of calcium channels by amyloids depends on the presence of anionic lipids. Our data showed that after the exposure of bacteria to space/Mars-like conditions, the amount of anionic PL increased.

Bacterial EVs are known to transfer out of cells misfolded proteins [50] formed under stressful conditions. Previously, in our study on the biological effects of the EVs originating from *K. oboediens* exposed to Mars-like stressors outside the ISS [20,21], we observed that the *E*-EVs had: 1) threatened membrane structure; 2) impaired the proton motive force transport of ions; 3) induced membrane-associated dehydrogenase activity. In addition, in this study, we showed that the E-EVs formed ion-channel-like pores in artificial eukaryotic membranes. Remarkably, after exposure to harsh conditions and changes in lipidome and proteome, practically no genomic changes have been revealed in the exposed IMBG185 [22]. We hypothesize that the impaired bacterial proteins or the appearance of prion-like proteins in bacteria under long-term exposure in the harsh hybrid environment probably caused a vertically transmissible protein aggregation known for bacteria [51]. These unidentified yet inheritable proteins probably get into the vesicles and are taken outside the bacterial cells. As we observed that the E-EVs built pores through the model bilayer membrane, we may assume that they carry misfolded proteins out from the cell and, in turn, these proteins promote negative curvature and build pores in the model planar membrane. This assumption should be confirmed in our future research.

5. Conclusion

Outer-membrane vesicles of the nonpathogenic bacterium *K. oboediens* acquired the capability to fuse the artificial eukaryotic membrane after exposure to hybrid space/Mars-like conditions simulated on the ISS. The most reliable fusion of the post-stress *E*-EVs was achieved with PC:PE:ergosterol or sterol-free PC:PE bilayers without conventional application of trans-bilayer osmotic gradient or one-sided addition of physiologically significant divalent cations. Reference EVs from ground-based bacteria never demonstrated a stable appreciable increase of transmembrane current as a marker of membrane fusion. The difference in membrane lipidome and content of aggregated proteins was clearly observed between homologous bacteria – exposed to the ISS and ground reference ones. More underlying physiological and pathological mechanisms should be explored to understand further the consequences of maintaining bacteria under harsh conditions.

CRediT authorship contribution statement

I. Orlovska: Conceptualization, Investigation, Methodology, Visualization. **G. Zubova:** Funding acquisition, Project administration. **O. Shatursky:** Investigation, Methodology, Visualization. **O. Kukharenko:** Investigation, Methodology, Visualization. **O. Podolich:** Data curation, Formal analysis. **T. Gorid'ko:** Investigation, Methodology, Visualization. **H. Kosyakova:** Investigation, Methodology, Visualization. **T. Borisova:** Resources, Writing – review & editing. **N. Kozyrovska:** Conceptualization, Supervision, Writing – original draft, Writing – review & editing.

Declaration of competing interest

The authors declare that they have no known competing financial interests or personal relationships that could have appeared to influence the work reported in this paper.

Acknowledgement

The authors thank Dr. K. Pyrshev for the excellent research on the fluorescence in membranes of bacterial vesicles, Dr. M. Galkin for DLS measurements, also Ms. M. Horbunova for technical assistance. Dr. Andrey Klymchenko (Directeur de recherche CNRS, Université de Strasbourg) and Dr. Oleksandr Kucherak (Ústav Organické Chemie a Biochemie AV ČR) are kindly acknowledged for providing the NR12S probe.

Funding

This work was supported by the National Academy of Sciences of Ukraine (grant 47/2022).

References

[1] M. Mathieu, L. Martin-Jaular, C. Théry, Specificities of secretion and uptake of exosomes and other extracellular vesicles for cell-to-cell communication, Nat. Cell Biol. 21 (2019) 9–17, https://doi.org/10.1038/s41556-018-0250-9.

[2] D.K. Jeppesen, Q. Zhang, J.L. Franklin, R.J. Coffey, Extracellular vesicles and nanoparticles: emerging complexities, Trends Cell Biol. (2023), https://doi.org/10.1016/j.tcb.2023.01.002 1.

[3] S. Gill, R. Catchpole, P. Forterre, Extracellular membrane vesicles in the three domains of life and beyond, FEMS Microbiol Reviews 43 (2019) 273–303, https://doi.org/10.1093/femsre/fuy042 (fuy042).

[4] M. Toyofuku, S. Schild, M. Kaparakis-Liaskos, L. Eberl, Composition and functions of bacterial membrane vesicles, Nat. Rev. Microbiol. (2023), https://doi.org/10.1038/s41579-023-00875-5.

[5] C. Zou, Y. Zhang, H. Liu, Y. Wu, X. Zhou, Extracellular vesicles: recent insights into the interaction between host and pathogenic bacteria, Front. Immunol. 13 (2022) 840550, https://doi.org/10.3389/fimmu.2022.840550.

[6] P. Aytar Çelik, K. Erdogan-Gover, D. Barut, B.M. Enuh, et al., Bacterial membrane vesicles as smart drug delivery and carrier systems: a new nanosystems tool for current anticancer and antimicrobial therapy, Pharmaceutics 15 (4) (2023) 1052, https://doi.org/10.3390/pharmaceutics15041052.

[7] R. Luo, Y. Chang, H. Liang, W. Zhang, et al., Interactions between extracellular vesicles and microbiome in human diseases: new therapeutic opportunities, iMeta (2023), https://doi.org/10.1002/imt2.86.

[8] Q. Shen, B. Xu, C. Wang, Y. Xiao, Y. Jin, Bacterial membrane vesicles in inflammatory bowel disease, Life Sci. 306 (2022) 120803, https://doi.org/10.1016/j.lfs.2022.120803.

[9] H. Liu, H. Zhang, Y. Han, H. Hu, et al., Bacterial extracellular vesicles-based therapeutic strategies for bone and soft tissue tumors therapy, Theranostics 12 (15) (2022) 6576–6594, https://doi.org/10.7150/thno.78034.

[10] Z. Huang, S. Keramat, M. Izadirad, Z.-S. Chen, M. Soukhtanloo, The potential role of exosomes in the treatment of brain tumors, recent updates and advances, Front. Oncol. 12 (2022) 869929, https://doi.org/10.3389/fonc.2022.869929.

[11] P.A. van der Ley, A. Zariri, E. van Riet, Oosterhoff D and Kruiswijk CP An intranasal OMV-based vaccine induces high mucosal and systemic protecting immunity against a SARS-CoV-2 infection, Front. Immunol. 12 (2021) 781280, https://doi.org/10.3389/fimmu.2021.781280.

[12] N. Krishnan, L.J. Kubiatowicz, M. Holay, J. Zhou, et al., Bacterial membrane vesicles for vaccine applications, Adv. Drug Deliv. Rev. 85 (2022) 114294, https://doi.org/10.1016/j.addr.2022.114294.

[13] N. Kozyrovska, O. Reva, O. Podolich, O. Kukharenko, I. Orlovska, V. Terzova, et al., To other planets with upgraded millennial Kombucha in rhythms of sustainability and health support, Front Astronom Space Sci 8 (2021) 701158, https://doi.org/10.3389/fspas.2021.701158.

[14] I. Orlovska, O. Podolich, O. Kukharenko, G. Zubova, et al., The conceptual approach to the use of postbiotics based on bacterial membrane nanovesicles for prophylaxis of astronauts' health disorders, Space Sci Technol 28 (6) (2022) 34–51, https://doi.org/10.15407/knit2022.06.034.

[15] L.A. Mulcahy, R.C. Pink, D.R.F. Carter, Routes and mechanisms of extracellular vesicle uptake, J Extracellular Vesicles 3 (2014) 24641, https://doi.org/10.3402/jev.v3.24641.

[16] J. Jäger, S. Keese, M. Roessle, M. Steinert, A.B. Schromm, Fusion of Legionella pneumophila outer membrane vesicles with eukaryotic membrane systems is a mechanism to deliver pathogen factors to host cell membranes, Cell. Microbiol. 17 (5) (2015) 607–620, https://doi.org/10.1111/cmi.12 392.

[17] S. Tarashi, M.S. Zamani, M.D. Omrani, A. Fateh, et al., Commensal and pathogenic bacterial-derived extracellular vesicles in host-bacterial and interbacterial dialogues: two sides of the same coin, J Immunol Res (2022) 8092170, https://doi.org/10.1155/2022/8092170 (15 pages).

[18] E.J. O'Donoghue, A.M. Krachler, Mechanisms of outer membrane vesicle entry into host cells, Cell. Microbiol. 18 (11) (2016) 1508–1517, https://doi.org/10.1111/cmi.12655.

[19] Y.M.D. Gnopo, A. Misra, H.L. Hsu, M.P. DeLisa, S. Daniel, D. Putnam, Induced fusion and aggregation of bacterial outer membrane vesicles: experimental and theoretical analysis, J. Colloid Interface Sci. 578 (2020) 522–532, https://doi.org/10.1016/j.jcis.2020.04.068.

[20] O. Podolich, O. Kukharenko, A. Haidak, I. Zaets, et al., Multimicrobial Kombucha culture tolerates Mars-like conditions simulated on low earth orbit, Astrobiology 19 (2) (2019) 183–196, https://doi.org/10.1089/ast.2017.1746.

[21] O. Podolich, O. Kukharenko, I. Zaets, I. Orlovska, et al., Fitness of outer membrane vesicles from Komagataeibacter intermedius is altered under the impact of simulated Mars-like stressors outside the International Space Station, Front. Microbiol. 11 (2020) 1268, https://doi.org/10.3389/fmicb.2020.01268.

[22] A. Góes-Neto, O. Kukharenko, I. Orlovska, O. Podolich, et al., Shotgun metagenomic analysis of Kombucha mutualistic community exposed to Mars-like environment outside the International Space Station, Environ. Microbiol. 23 (7) (2021) 3727–3742, https://doi.org/10.1111/1462-2920.15405.

[23] S. Hestrin, M. Schramm, Synthesis of cellulose by Acetobacter xylinum. 2. Preparation of freeze-dried cells capable of polymerizing glucose to cellulose, Biochem. J. 58 (1954) 345–352, https://doi.org/10.1042/bj0580345.

[24] V.E. Vaskovsky, E.Y. Kostetsky, I.M. Vasendin, A universal reagent for phospholipid analysis, J. Chromatogr. 114 (1975) 129–141, https://doi.org/10.1016/S0021-9673(00)85249-8.

[25] M.S. Perin, R.C. MacDonald, Fusion of synaptic vesicle membranes with planar bilayer membranes, Biophys. J. 55 (1989) 973, https://doi.org/10.1016/S0006-3495(89)82896-6.

[26] Shatursky OYa, Demchenko AP, Panas I, Krisanova N, et al. The ability of carbon nanoparticles to increase transmembrane current of cations coincides with impaired synaptic neurotransmission, Biochim Biophys-Biomembranes, 2022, 1864(1), doi:https://doi.org/10.1016/j.bbamem. 2021.183817.

[27] O.A. Kucherak, S. Oncul, Z. Darwich, D.A. Yushchenko, et al., Switchable nile red-based probe for cholesterol and lipid order at the outer leaflet of biomembranes, J. Am. Chem. Soc. (2010), https://doi.org/10.1021/ja100351w (7,132(13),4907-4916).

[28] K.A. Pyrshev, S.O. Yesylevskyy, A.P. Demchenko, Double-exponential kinetics of binding and redistribution of the fluorescent dyes in cell membranes witness for the existence of lipid microdomains, Biochem. Biophys. Res. Commun. 508 (2019) 1139–1144. ISSN 0006-291X,, https://doi.org/10.1016/j.bbrc.2018.12.054.

[29] H. Naiki, K. Higuchi, M. Hosokawa, T. Takeda, Fluorometric determination of amyloid fibrils in vitro using the fluorescent dye, thioflavine T, Anal. Biochem. 177 (1989) 244–249, https://doi.org/10.1016/0003-2697(89)90046-8.

[30] D.J. Woodbury, C. Miller, Nystatin-induced liposome fusion: a versatile approach to ion channel reconstitution into planar bilayers, Biophys. J. 58 (1990) 833–839, https://doi.org/10.1016/S0006-3495(90)82429-2.

[31] J.P. Sáenz, D. Grosser, A.S. Bradley, T.J. Lagny, et al., Hopanoids as functional analogues of cholesterol in bacterial membranes, PNAS 112 (38) (2015) 11971–11976, https://doi.org/10.1073/pnas.15 15607112.

[32] Bogdanov M, Pyrshev K, Yesylevskyy S, Ryabichko S. Phospholipid distribution in the cytoplasmic membrane of Gram-negative bacteria is highly asymmetric, dynamic, and cell shape-dependent Sci. Adv.6,eaaz6333(2020).DOI:https://doi.org/10.1126/sciadv.aaz6333.

[33] A.P. Galkin, E.I. Sysoev, Stress response is the main trigger of sporadic amyloidoses, Int. J. Mol. Sci. 22 (8) (2021) 4092, https://doi.org/10.3390/ijms22084092.

[34] F.D. Schramm, K. Schroeder, K. Jonas, Protein aggregation in bacteria, FEMS Microbiol. Rev. fuz026, 44 (2020) 54–72, https://doi.org/10.1093/femsre/fuz026.

[35] Y.M.D. Gnopo, D. Putnam, A lipid mixing assay to accurately quantify the fusion of outer membrane vesicles, Methods 1 (177) (2020) 74–79, https://doi.org/10.1016/j.ymeth.2019.11.009.

[36] A. Joardar, G.P. Pattnaik, H. Chakraborty, Mechanism of membrane fusion: interplay of lipid and peptide, J. Membr. Biol. 255 (2022) 211–224, https://doi.org/10.1007/s00232-022-00233-1.

[37] M.C. Mansilla, L.I. Cybulski, D. Albanesi, D. de Mendoza, Control of membrane lipid fluidity by molecular thermosensors, J. Bacteriol. 186 (20) (2004) 6681–6688, https://doi.org/10.1128/JB.186.20.6681-6688.2004.

[38] B. Mostofian, T. Zhuang, X. Cheng, J.D. Nickels, Branched-chain fatty acid content modulates structure, fluidity, and phase in model microbial cell membranes, J. Phys. Chem. B 123 (2019) 5814–5821, https://doi.org/10.1021/acs.jpcb.9b04326.

[39] M. Gohrbandt, A. Lipski, J.W. Grimshaw, et al., Low membrane fluidity triggers lipid phase separation and protein segregation in living bacteria, The EMBO J 41 (2022) e109800, https://doi.org/10.15252/embj.2021109800.

[40] E.L. Dulaney, E.O. Stapley, K. Simf, Studies on ergosterol production by yeasts, Appl. Microbiol. 2 (1954) 371–379, https://doi.org/10.1128/am.2.6.371-379.1954.

[41] G.P. Pattnaik, G. Meher, H. Chakraborty, Exploring the mechanism of viral peptide-induced membrane fusion, Adv. Exp. Med. Biol. 1112 (2018) 69–78, https://doi.org/10.1007/978-981-13-3065-0_6.

[42] F. Tsigelny, Y. Sharikov, M.A. Miller, E. Masliah, Molecular mechanism of pore creation in bacterial membranes by amyloid proteins, J. Phys. Conf. Ser. 180 (2009) 012026, https://doi.org/10.1088/1742-6596/180/1/012026.

[43] Di Scala C, Yahi N, Boutemeur C, Flores A, Rodri et al. Common molecular mechanism of amyloid pore formation by Alzheimer's β-amyloid peptide and α-synuclein. Sci. Rep. 2016, 6: 28781. doi:https://doi.org/10.1038/srep28781.

[44] M.F.M. Sciacca, C. La Rosa, D. Milardi, Amyloid-mediated mechanisms of membrane disruption, Biophysica 1 (2) (2021) 137–156, https://doi.org/10.3390/biophysica1020011.

[45] J. Krausser, T.P.J. Knowles, A. Šarić, Physical mechanisms of amyloid nucleation on fluid membranes, PNAS 117 (52) (2020) 33090–33098, https://doi.org/10.1073/pnas.2007694117.

[46] C. Fernández, R. Núñez-Ramírez, M. Jiménez, G. Rivas, R. Giraldo, RepA-WH1, the agent of an amyloid proteinopathy in bacteria, builds oligomeric pores through lipid vesicles, Sci. Rep. 6 (2016) 23144, https://doi.org/10.1038/srep23144.

[47] N.G. Bednarska, J. Schymkowitz, F. Rousseau, J. Van Eldere, Protein aggregation in bacteria: the thin boundary between functionality and toxicity, Microbiology 159 (2013) 1795–1806, https://doi.org/10.1099/mic.0.069575-0.

[48] L. Molina-García, M. Moreno-del Álamo, P. Botias, Z. Martín-Moldes, et al., Outlining core pathways of amyloid toxicity in bacteria with the RepA-WH1 prionoid, Front. Microbiol. 8 (2017) 539, https://doi.org/10.3389/fmicb.2017.00539.

[49] Kukharenko OYe, Terzova VO, Zubova GV. Protein aggregates carry non-genetic memory in bacteria after stresses. Biopolym Cell, 2020, 36(6), 409–422. doi:https://doi.org/10.7124/bc.000A3F.

[50] A.J. McBroom, M.J. Kuehn, Release of outer membrane vesicles by Gram-negative bacteria is a novel envelope stress response, Mol. Microbiol. 63 (2) (2007) 545–558, https://doi.org/10.1111/j.1365-2958.2006.05522.x.

[51] S.K. Govers, J. Mortier, A. Adam, A. Aertsen, Protein aggregates encode epigenetic memory of stressful encounters in individual Escherichia coli cells, PLoS Biol. 16 (8) (2018) e2003853, https://doi.org/10.1371/journal.pbio.2003853.